

Noncrossing simultaneous Bayesian quantile curve fitting

T. Rodrigues^{*†} J.-L. Dortet-Bernadet[‡] and Y. Fan^{* §}

Abstract

Bayesian simultaneous estimation of nonparametric quantile curves is a challenging problem, requiring a flexible and robust data model whilst satisfying the monotonicity or noncrossing constraints on the quantiles. This paper presents the use of the pyramid quantile regression method in the spline regression setting. In high dimensional problems, the choice of the pyramid locations becomes crucial for a robust parameter estimation. In this work we derive the optimal pyramid locations which then allows us to propose an efficient adaptive block-update MCMC scheme for posterior computation. Simulation studies show the proposed method provides estimates with significantly smaller errors and better empirical coverage probability when compared to existing alternative approaches. We illustrate the method with three real applications.

Keywords: Bayesian quantile pyramid; Simultaneous quantile regression; B-Splines; O’Sullivan penalised splines; Nonparametric quantile regression.

^{*}School of Mathematics and Statistics, University of New South Wales, Sydney 2052 Australia.

[†]CAPES Foundation, Ministry of Education of Brazil, Brasília - DF 70040-020, Brazil

[‡]Institut de Recherche Mathématique Avancée, UMR 7501 CNRS, Université de Strasbourg, Strasbourg, France.

[§]Communicating Author: Y.Fan@unsw.edu.au

1 Introduction

Quantile regression models (QR; Koenker and Bassett 1978) provide a comprehensive description of the conditional distribution of the response variable by capturing the effect of covariates at different quantile levels. It is a robust alternative to ordinary mean regression and has been embraced by a variety of fields, including biology, economics, environmental sciences, medicine and ecology (Fitzenberger et al. 2002, Reich et al. 2011, Portnoy 2003, Cade et al. 1999). For modelling the τ -th conditional quantile curve of a response variable Y given the value $X = x$ of some covariate X as $Q_\tau(Y|x) = f_\tau(x)$, $\tau \in (0, 1)$, consider

$$Y|X = x \sim f_\tau(x) + \epsilon,$$

where the error variable ϵ satisfies $Q_\tau(\epsilon|x) \equiv \inf\{a : P(\epsilon \leq a|X = x) \geq \tau\} = 0$, and the function $f_\tau(x)$ changes with τ and describes the relationship between X and Y . In this article, we are interested in the case where the curve f_τ is modeled with spline functions of a given degree, $P \geq 1$, so that,

$$f_\tau(x) = \alpha_0 + \sum_{j=1}^P \alpha_j x^j + \sum_{k=1}^K \eta_k (x - \gamma_k)_+^P \quad (1)$$

where $z_+ = \max(0, z)$ and where $\gamma_k, k = 1, \dots, K$, represent the locations of K knot points (see Hastie and Tibshirani 1990). Typically, the degree P is set to 3, since cubic splines are known to approximate locally smooth functions sufficiently well.

Frequentist literature on quantile regression is largely based on the seminal work by Koenker and Bassett (1978), in which the noise distribution is left unspecified and quantiles are estimated by solving the linear optimisation problem

$$\widehat{Q}_\tau(Y|x) = \arg \min_{f_\tau(x)} \sum_{i=1}^n \rho_\tau(y_i - f_\tau(x_i)), \quad (2)$$

where $\rho_\tau(\cdot)$ is an asymmetric loss function given by $\rho_\tau(\epsilon) = \tau\epsilon$ if $\epsilon \geq 0$, and $\rho_\tau(\epsilon) = (\tau - 1)\epsilon$ otherwise. In the spline fitting context, a penalty term is added to (2) in order to restrict the class of functions $f_\tau(x)$ to be sufficiently smooth. However, the simplicity of linear programming is jeopardised when the classical quadratic penalty, $L_2 = \int (f''(x))^2 dx$, is added to this objective function (Bosch et al. 1995). Koenker et al. (1994) advocate the use of a linear norm under the total variation roughness penalty, $L_1 = \int |(f''(x))| dx$, nevertheless one becomes harshly delimited by the space of piecewise linear fits. On the other hand, under the scope of linear programming, extension to quadratic splines is still possible when using the L_∞ -norm, $L_\infty = \sup |f''(x)|$, see *e.g.* Koenker et al. (1994) or He and Ng (1999). In the Bayesian framework, the need for a likelihood specification was initially accommodated by the asymmetric Laplace error model introduced by Yu and Moyeed (2001a), based on its analogy to the minimisation problem (2). Smoothing cubic splines can be easily incorporated considering a prior density for $f_\tau(x)$ proportional to $\exp\{-\frac{1}{2}\lambda \int f''(x)^2 dx\}$ (see Thompson et al. 2010).

However, one common issue facing these approaches is that quantiles at different levels have to be fitted singly for each τ and final estimates may cross, *ie.* estimates may not respect the monotonicity of the quantile function. In the context of nonparametric regression, the flexibility granted to the quantile curves makes crossing more severe. Post-processing procedures (*e.g.* Dette and Volgushev 2008, Chernozhukov et al. 2009) which correct for crossing still suffer from a poor borrowing of information, and can still lead to wildly variable curves across quantile levels τ . Rodrigues and Fan (2017) proposed a procedure to postprocess crossing quantiles in a Bayesian framework, however its performance is still influenced by the initial estimates. Recently, several authors have argued that simultaneous estimation offers better estimates, better global efficiency for the estimators have been observed empirically in several studies (Reich and Smith 2013, Yang and Tokdar 2017, Fang et al. 2015, Rodrigues et al. 2016). Indeed simultaneous quantile fitting is a challenging problem that has gained a lot of attention in recent times. A so-

lution to the constrained minimisation problem was proposed by Bondell et al. (2010), however estimation is again limited to piecewise linear fits. One can also achieve non-crossing by restricting the class of models to the location-scale family (He 1997), or by minimising the objective function sequentially while imposing ordering through the parameters (Muggeo et al. 2013), but there are naturally limitations when rigid assumptions are imposed. More recently, Yang and Tokdar (2017) proposed a Bayesian model for joint estimation of quantile planes using a convenient parameterisation to facilitate the incorporation of monotonicity constraints. Although its focus is linear regression, shrinkage priors for variable selection could potentially be used for fitting splines.

Pyramid quantile regression was first presented in Rodrigues et al. (2016) as an alternative Bayesian procedure for simultaneous quantile fitting. This approach compared favourably with competing methods in empirical studies. It relies on the use of several so-called quantile pyramid priors introduced by Hjort and Walker (2009) placed at some chosen locations in the covariate space. By construction this method ensures non-crossing of the different quantile planes within the convex hull of the pyramid locations. Although the spline regression model (1) can be estimated under the linear regression umbrella, the pyramid quantile regression when a large number of basis functions are used can be problematic. As a matter of fact, the choice of pyramid locations is intricate in this situation since standard convex hull algorithms either cannot cope with high-dimensional spaces or return too many vertices. This complicates estimation, as crossing of quantile curves will need to be checked at many locations for each parameter update of an MCMC sampling algorithm.

In this paper, we propose a method based on the pyramid quantile regression for simultaneously fitting several penalised spline quantile curves which automatically satisfy the non-crossing constraints. In order to achieve that, we propose to enclose the data cloud with a polytope whose number of vertices equals the number of parameters in the regression spline model, and we derive a general algorithm to find the optimal vertex

locations of this convex set, efficiently eliminating all monotonicity constraints. As far as we are aware, there are no existing algorithms in the convex optimisation literature which can compute such vertices. Our approach here is also scalable to high dimensions. Next, we develop penalty criteria for estimating flexible quantile curves, and propose an efficient adaptive block-update strategy for MCMC sampling, taking advantage of the proposed convex polytope approach.

The rest of the article is organised as follows. Section 2 presents the optimal convex set enclosing the data cloud with the given number of vertices. Section 3 recalls some basics on quantile pyramids introduced by Hjort and Walker (2009) and briefly describe their use in Rodrigues et al. (2016) in a regression set-up. In Section 4 we introduce the penalised quantile splines model and describe the modelling set up. Section 5 presents simulation studies and comparisons with the best alternative approaches. Several real datasets are analysed in section 6, and concluding remarks are discussed in the final section.

2 Convex set vertices

The convex hull of the predictor cloud has a special role in simultaneous linear quantile regression. It is well known that if the conditional quantiles do not cross at the vertices of a convex set, they do not cross anywhere inside the convex set, see for example Bondell et al. (2010). This fact reduces the problem of infinite quantile monotonicity constraints to ensuring monotonicity only at the vertices of the convex set. Rodrigues et al. (2016) used quantile pyramids at selected vertices of the convex hull of the predictor cloud, non-crossing conditions being checked at the remaining vertices. However, in practice, convex hulls of datapoints in dimensions higher than 9 or 10 can be difficult to obtain, and when an algorithm is successful at doing so it may return a large number of vertices. In these cases, it may be better to work with a larger convex set which gives fewer vertices and, consequently, reduced constraints. Nevertheless, some caution needs to be taken when imposing noncrossing constraints on a too large simplex, as it can result in parallel

quantile planes (see Yang and Tokdar 2017). This point is particularly relevant when covariates are correlated.

The spline regression model (1), viewed as a multiple linear regression model, is an example of such a difficult situation. Here the predictor data cloud lies on a one-dimensional curve, say \mathcal{X} , in the high dimensional space \mathbb{R}^{K+P+1} and the number of vertices of the convex hull of this predictor data cloud is the entire data set. To avoid all the abovementioned problems the following proposition gives, for the cubic case $P = 3$, the optimal convex set with $K + 4$ vertices that contains the curve \mathcal{X} (see Appendix for a proof).

Proposition 1. *Without loss of generality, suppose the covariate x lies in $(0, 1)$. Consider a cubic polynomial splines basis with K internal knots denoted by $0 < \gamma_1 < \gamma_2 < \dots < \gamma_K < 1$. The minimum volume convex set with $K + 4$ vertices that encompasses the curve \mathcal{X} is a polytope in \mathbb{R}^{K+3} with the following vertices:*

$$\begin{aligned}
x^1 &= (0, 0, 0, 0, 0, \dots, 0) \\
x^2 &= (\frac{1}{2}, 0, 0, 0, 0, \dots, 0) \\
x^3 &= (\frac{2}{3}, \frac{1}{3}, 0, 0, 0, \dots, 0) \\
x^4 &= (\frac{2+\gamma_1}{3}, \frac{1+2\gamma_1}{3}, \gamma_1, 0, 0, \dots, 0) \\
x^5 &= (\frac{2+\gamma_2}{3}, \frac{1+2\gamma_2}{3}, \gamma_2, (\gamma_2 - \gamma_1)(1 - \gamma_1)^2, 0, \dots, 0) \\
x^6 &= (\frac{2+\gamma_3}{3}, \frac{1+2\gamma_3}{3}, \gamma_3, (\gamma_3 - \gamma_1)(1 - \gamma_1)^2, (\gamma_3 - \gamma_2)(1 - \gamma_2)^2, 0, \dots, 0) \\
x^7 &= (\frac{2+\gamma_4}{3}, \frac{1+2\gamma_4}{3}, \gamma_4, (\gamma_4 - \gamma_1)(1 - \gamma_1)^2, (\gamma_4 - \gamma_2)(1 - \gamma_2)^2, (\gamma_4 - \gamma_3)(1 - \gamma_3)^2, 0, \dots, 0) \\
&\dots \\
x^{K+3} &= (\frac{2+\gamma_K}{3}, \frac{1+2\gamma_K}{3}, \gamma_K, (\gamma_K - \gamma_1)(1 - \gamma_1)^2, (\gamma_K - \gamma_2)(1 - \gamma_2)^2, \dots, (\gamma_K - \gamma_{K-1})(1 - \gamma_{K-1})^2, 0) \\
x^{K+4} &= (1, 1, 1, (1 - \gamma_1)^3, (1 - \gamma_2)^3, \dots, (1 - \gamma_K)^3)
\end{aligned}$$

Figure 6 in the Appendix illustrates the choice of the vertex locations for the first elements of the cubic polynomial spline basis, $\{1, x, x^2\}$ and $\{1, x, x^2, x^3\}$. The correspond-

ing convex hull are the shaded regions enclosing, as narrowly as possible, the curves $\{(x, x^2), x \in (0, 1)\}$ and $\{(x, x^2, x^3), x \in (0, 1)\}$. The choice of fixed $K + 4$ vertices is related to our modelling framework (detailed in the next sections) and reflects the spline curve degree of freedom. Proposition 1 can of course also be used with other modelling setups to ensure non-crossing.

Proposition 1 provides the vertices with respect to the cubic polynomial spline basis. For B-splines basis functions, a transformation of basis can be applied to the aforementioned vertices to find the corresponding ones in the new coordinate system (see Ruppert et al. (2003) and Spiriti et al. (2013)). Although the same fit is obtained with both basis, in many applications, the B-spline basis are preferred for computational reasons and will be used in this paper. More specifically, we replace Equation (1) with cubic B-splines to nonparametrically model the quantile curve,

$$f_{\tau}(x) = \sum_{j=1}^{K+4} \theta_{\tau}^j B_j(x), \quad (3)$$

where $B_j(x)$, $j = 1, \dots, K + 4$, are the B-splines basis functions with K internal knots, and θ_{τ}^j denotes the corresponding j th coefficient for the τ th quantile curve. The corresponding vertex locations under the B-splines basis are easily obtained by a simple linear mapping corresponding to the change of basis, see Ruppert et al. (2003). In the next sections, we will describe our modelling approach for the simultaneous penalised quantile spline curves.

3 Quantile pyramids

Here we provide some background on quantile pyramids, which was introduced by Hjort and Walker (2009). Quantile pyramid is a method for constructing a random probability measure via the quantile function. We will use hereafter these priors for simultaneous inference on quantile spline curves, in the spirit of the linear quantile regression model

recently proposed in Rodrigues et al. (2016).

Quantile pyramid is a tree generation process with M levels where, at each level m , quantiles for fixed probabilities τ_{mj} , $j = 1, 2, \dots, 2^{m-1}$, are randomly generated. Consider first that the process starts with $Q_0 = 0$ and $Q_1 = 1$, so that the quantile pyramid defines a random distribution on $[0, 1]$. Then, the sampling order of the set of given quantile levels $\tau_1 < \tau_2 < \dots < \tau_T$ is defined as follows. At $m = 1$, we draw a single quantile $Q_{\tau_{11}}$, whose level τ_{11} is halfway into this set of given levels. Now let τ_{mj}^L and τ_{mj}^R be the closest left and right ancestors of the next quantile level to be drawn τ_{mj} (ie. antecessors whose quantile levels are adjacent to τ_{mj}). So for the subsequent levels ($m > 2$), we draw quantiles $Q_{\tau_{mj}}$, where τ_{mj} is chosen as the middle level between τ_{mj}^L and τ_{mj}^R . If there is an even number of quantile levels to split, for identification purposes, we take the middle value to be the smallest level. The process stops at a finite level M , when all quantile levels of interest have been sampled, and the random quantile function is obtained by linear interpolation on the set of quantiles Q_{τ_t} , $t = 1, \dots, T$.

Regarding the random generation process of quantile $Q_{\tau_{mj}}$, this is dictated by

$$Q_{\tau_{mj}} = Q_{\tau_{mj}^L} (1 - V_{mj}) + Q_{\tau_{mj}^R} V_{mj}, \quad (4)$$

where V_{mj} is a random variable on $(0, 1)$ that defines the weights of the averaging process at level m . Following Hjort and Walker (2009) and Rodrigues et al. (2016), we assume that $V_{mj} \sim \text{Beta}(a_{mj}, b_{mj})$, with $a_{mj} = 2m$ and expected value given by

$$E(V_{mj}) = \frac{\tau_{mj} - \tau_{mj}^L}{\tau_{mj}^R - \tau_{mj}^L}. \quad (5)$$

This describes a quantile process centred on a standard Uniform distribution, denoted thereafter as Q_{τ}^{unif} , where the variance of the variables V_{mj} decreases with m .

Furthermore, one can centre the quantile process in any distribution with cdf F by

applying the following transformation

$$Q_\tau = F^{-1}(Q_\tau^{unif}). \quad (6)$$

Therefore, prior knowledge about the distributional form of the data can be incorporated into the model via F . Here we will consider data arising from the reals and use as default centring choice the Gaussian distribution.

The simultaneous prior density for the quantiles can be expressed as

$$\pi(Q_{\tau_1}, \dots, Q_{\tau_T}) = \prod_{m=1}^M \prod_{j=1}^{2^{m-1}} \pi_{mj}(Q(\tau_{mj}) \mid Q(\tau_{mj}^L), Q(\tau_{mj}^R)), \quad (7)$$

where the conditional densities π_{mj} are derived from the transformation of variables given in Equations (4) and (6), and considering $V_{mj} \sim \text{Beta}(a_{mj}, b_{mj})$. Samples from this quantile process are then piecewise Normal quantile functions. For further details, we refer to Hjort and Walker (2009). In particular they give conditions for the Bayesian consistency of the procedure when one uses as prior on the distribution of the data a quantile pyramid with infinite level $M = +\infty$.

The pyramid quantile regression model described in Rodrigues et al. (2016) uses these pyramid quantile priors in a regression setting. In short, independent pyramid quantile placed at different locations of the predictor space define the quantile planes. This offers a method for simultaneous inference on the quantile planes, that are by nature non crossing on the convex hull of the pyramid locations. We refer also to this article for a discussion on the posterior consistency of the procedure.

4 Quantile Pyramids for Penalised Splines

The proposed model for simultaneously fitting penalised splines using quantile pyramids is discussed in this section. We consider jointly modelling quantile curves, for a number

T of finite quantile levels $\tau = \tau_1 < \tau_2 < \dots < \tau_T$, as a function of a covariate $x \in \mathbb{R}$.

4.1 Model formulation

For given quantile levels τ , we consider the use of cubic splines to the model quantile curves. Denote the K internal knots as $\gamma_1 = \gamma_2 = \gamma_3 = \gamma_4 < \gamma_5 < \dots < \gamma_{K+4} < \gamma_{K+5} = \gamma_{K+6} = \gamma_{K+7} = \gamma_{K+8}$, so that $Q_\tau(Y|x) = \sum_{j=1}^{K+4} \theta_j^j B_j(x)$, where B_1, \dots, B_{K+4} are the B-splines basis functions defined by these knots. For each τ , such linear combinations can be seen as a hyperplane in \mathbb{R}^{K+4} , and represented as an affine combination of $K+4$ points $Q_\tau(y|x^p)$, or in short Q_τ^p , located at distinct locations $x^p \in \mathbb{R}^{K+4}$, $p = 1, \dots, K+4$, that is,

$$Q_\tau(Y|x) = \sum_{p=1}^{K+4} Q_\tau^p M_p(x) = \mathbf{Q}_\tau^p \mathbf{M}, \quad (8)$$

where the design matrix \mathbf{M} can be obtained from $\mathbf{M} = (\mathbf{Q}_\tau^p)^{-1} \mathbf{Q}_\tau(Y|x)$, for arbitrary points \mathbf{Q}_τ^p and the corresponding quantiles $\mathbf{Q}_\tau(Y|x_i)$, $i = 1, \dots, n$.

Since model (8) is parameterised in terms of the quantiles Q_τ^p , we consider using $K+4$ separate quantile pyramids to represent the prior quantile processes at each x^p location. We use as the pyramid locations the vertices of the convex hull given in Proposition 1. This ensures that the hyperplanes that passes through these points at varying quantile levels τ will not cross inside the convex hull, thereby producing non-crossing regression splines without any additional need to check for non-crossing during computation.

Assuming pyramid priors centred on the Normal distribution, the corresponding likelihood is formulated as a piecewise Normal density

$$f(y|x) = \sum_{t=1}^T (\tau_t - \tau_{t-1}) \frac{\phi(y; \mu_x, \sigma_x^2)}{\Phi\left(\frac{Q_{\tau_t}(Y|x) - \mu_x}{\sigma_x}\right) - \Phi\left(\frac{Q_{\tau_{t-1}}(Y|x) - \mu_x}{\sigma_x}\right)} I_{(Q_{\tau_t}(Y|x), Q_{\tau_{t-1}}(Y|x)]}(y), \quad (9)$$

where $I_{(q_1, q_2]}(y)$ is 1 if $y \in (q_1, q_2]$ and zero otherwise, and $\phi(\cdot; \mu_x, \sigma_x^2)$ denotes the density function of the centring Normal distribution $\mathcal{N}(\mu_x, \sigma_x^2)$, where the centring mean μ_x

and the centring standard deviation σ_x can vary with x . We describe how to specify the centring parameters and penalisation in the next sections.

4.2 Penalised centring mean

For nonlinear curve fitting, we consider allowing the centring mean μ_x to also vary flexibly and smoothly with x . To achieve this, we assume that the mean curve of the centring distribution is a cubic B-spline with the same set of knots γ , ie. $\mu_x = \sum_{j=1}^{K+4} \eta_j B_j(x) = \boldsymbol{\eta} \mathbf{B}$, as for the quantiles. It is well known that the number and location of knots in spline based regression models play an important role in obtaining a good fit. Here we use a large number of knots K , and penalise the centring mean curve to obtain smoothness. Note that by constraining the mean and variance parameters of the centring distribution to vary smoothly across x , we obtain smoothness for the entire centring distributions (ie. all centring quantiles).

In order to avoid rank deficient covariance matrix and facilitate the incorporation of more complex models, we use the O'Sullivan penalised splines. See Wand and Ormerod (2008) for a discussion on the differences between P-splines and smoothing splines. Their mixed model formulation is considered here,

$$\mu_x = \mathbf{X}\boldsymbol{\beta} + \mathbf{Z}\mathbf{u} , \quad (10a)$$

$$\mathbf{u} \sim \mathcal{N}(\mathbf{0}, \sigma_u^2 \mathbf{I}) , \quad (10b)$$

with design matrices $\mathbf{X}_{(N \times 2)} = [1, x_i]_{1 \leq i \leq n}$ and $\mathbf{Z}_{(N \times (K+2))} = \mathbf{B}\mathbf{U}_Z \text{diag}(\mathbf{d}_Z^{-1/2})$, for the fixed and random effects, respectively. In order to obtain \mathbf{U}_Z and \mathbf{d}_Z , consider the $(K+4) \times (K+4)$ penalty matrix $\boldsymbol{\Omega}$, whose entries are $\Omega_{kk'} = \int_a^b B_k''(x) B_{k'}''(x) dx$, and take its spectral decomposition $\boldsymbol{\Omega} = \mathbf{U} \text{diag}(\mathbf{d}) \mathbf{U}^T$. Here $\mathbf{U}^T \mathbf{U} = \mathbf{I}$, and \mathbf{d}_Z is the $(K+2)$ sub-vector of \mathbf{d} containing its positive entries, whereas \mathbf{U}_Z is the $(K+4) \times (K+2)$ sub-matrix of \mathbf{U} with columns corresponding to the positive entries of \mathbf{d} . For further details, including

codes, see Wand and Ormerod (2008). Following their suggestions, we adopt throughout the paper standard non-informative priors for the additional parameters β and σ_u^2 , $\beta_0 \sim \mathcal{N}(0, 10^8)$, $\beta_1 \sim \mathcal{N}(0, 10^8)$ and $\sigma_u^2 \sim IG(0.01, 0.01)$, but results are not sensitive to these choices.

4.3 Centring standard deviation

A simpler cubic B-splines is considered for modelling the standard deviation of the centring distribution, as generally the variability function has less fluctuation and complexity. Therefore, we consider $\sigma_x = \sum_{j=1}^{R+4} \nu_j B_j(x)$, where R is a reduced number of interior knots. Using the hyperplane parameterisation we have

$$\sigma_x = \sum_{p=1}^{R+4} \sigma^p N_p(x) = \boldsymbol{\sigma}^p \mathbf{N}, \quad (11)$$

where \mathbf{N} is the corresponding design matrix and $\boldsymbol{\sigma}^p$ is a vector containing the standard deviations at $(R + 4)$ pyramids. Independent uniform priors were adopted for the standard deviations, $\sigma^p \sim U(0.01, 10^6)$, and $R = 3$ internal knots were used for all simulations and applications, providing sufficient flexibility for the variability curves.

4.4 Model fitting

Based on these prior specifications, the proposed model can be summarized as follows

$$Y|x \sim pw\mathcal{N}(\mathbf{Q}_{\tau_t, t=1:T}(Y|x), \mu_x, \sigma_x) \quad (12a)$$

$$Q_{\tau_t}(Y|x) = \mathbf{Q}_{\tau_t}^p \mathbf{M}, \quad \forall t = 1, \dots, T \quad (12b)$$

$$\mu_x = \mathbf{X}\boldsymbol{\beta} + \mathbf{Z}\mathbf{u}, \quad \mathbf{u} \sim \mathcal{N}(\mathbf{0}, \sigma_u^2 \mathbf{I}) \quad (12c)$$

$$\sigma_x = \boldsymbol{\sigma}^p \mathbf{N} \quad (12d)$$

where $pw\mathcal{N}(\mathbf{Q}_{\tau_t, t=1:T}(Y|x), \mu_x, \sigma_x)$ is the distribution with piecewise Normal density (9), whose parameters μ_x and σ_x are functions of covariate x . More specifically, quantiles $Q_{\tau_t}(Y|x)$ are cubic B-splines with K knots (12b), mean function μ_x is a penalised cubic B-spline (12c), and σ_x is a cubic B-spline with reduced R knots (12d). And with respect to the prior choices, quantile pyramid is considered for $Q_{\tau_t}(Y|x)$, whereas for the other parameters we use $\beta_0, \beta_1 \sim \mathcal{N}(0, 10^8)$, $\sigma_u^2 \sim IG(0.01, 0.01)$, $\sigma^p \sim U(0.01, 10^6)$.

Model inference is based on running Markov Chain Monte Carlo over the parameter vector $(\mathbf{Q}_{\tau_t}^p, \boldsymbol{\beta}, \mathbf{u}, \sigma_u^2, \sigma^p)$, whose elements have dimensions $(K + 4) \times T, 2, (K + 2), 1, R + 4$, respectively. When the number of covariates is large, parameters become highly correlated and more advanced MCMC techniques become necessary. Placing quantile pyramids at the convex hull vertices produces non-crossing planes by construction, this also means that constructing an adaptive MCMC algorithm in which we make use of parameter correlation structure is now feasible. It turns out that learning the correlation is crucial to MCMC performance. We propose to do this in a two stage procedure. In a first stage, parameters are updated one at a time using the Metropolised Gibbs sampling. Proposal distributions for quantiles $\mathbf{Q}_{\tau_t}^p$ are Uniform, and for the remaining parameters are Gaussian, all centred on the current value of the chain. A Robbins-Monro search scheme algorithm detailed in Garthwaite et al. (2016) is used to automatically tune the scaling parameters of these proposal distributions in order to achieve the optimal acceptance rate of 0.44 (Roberts and Rosenthal 2001). The covariance structure among model parameters is estimated based on the first stage sampling, and hierarchical clustering is performed to create blocks based on this posterior correlation (using Blocks function from R-package LaplacesDemon, Statisticat and LLC. 2016). Then, in a second stage, block-wise Metropolis-Hastings is performed using a multivariate Normal proposal distribution, with previously estimated posterior correlation matrix. Again, we consider the algorithm of Garthwaite et al. (2016) to tune the scaling in order to achieve the multivariate optimal acceptance rate of 0.23 (Roberts et al. 1997). Parameter estimates are then

calculated considering the posterior mean of the chain.

5 Simulated examples

In this section we examine the performances of the proposed method *via* a simulation study. We compare its results with the ones obtained by recent alternative approaches with available codes. This includes constrained B-splines smoothing (COBs), which provides individual quantile fittings using quadratic splines with L_∞ penalty, available in the R package `cobs`, see Ng and Maechler (2015) and Ng and Maechler (2007). This includes also the simultaneous quantile curve estimation available from the `gcqr` function of the `quantregGrowth` R-package (Muggeo et al. 2013), which provides cubic p-splines with L_2 penalty. Here standard errors of the estimates under this method were calculated using 100.000 bootstrap samples.

In the Bayesian framework, Yang and Tokdar (2017) recently proposed a model for joint estimation of quantile planes (QRJ from R-package `qrjoint`, Tokdar 2016). QRJ estimates were obtained here using 40.000 MCMC samples, thinning every 10 samples and discarding the initial 20% of the samples as burn-in, also τ increment was set to 0.001. Although QRJ primary focus is linear regression, the authors point out that their modelling platform is broad and discuss the use of shrinkage priors for variable selection. Therefore, we attempted here to use B-spline transform of the covariate variable as linear predictor in the regression model, and applied the suggested shrinkage priors (horseshoe prior for γ_0 and γ , and a spike-slab mixture of gamma for κ).

Estimates from the method presented in this paper, pyramid quantile penalised splines (PQPS), are obtained from an adaptive Markov chain Monte Carlo sampler. The underlying covariance structure is estimated considering 60.000 MCMC draws and burn-in of 10.000. Thereafter blockwise sampling is performed with 200.000 MCMC draws, thinning every 10 samples, and 10.000 burn-in. For all aforementioned approaches we consider fitting a B-spline curve with 20 knots spread evenly across covariate values.

Codes for fitting noncrossing splines regression quantiles (NCRQ) by solving a constrained minimisation problem (Bondell et al. 2010) are not available, so we included here the nonparametric simulation designs proposed by them to have their results for comparison. NCRQ fits linear splines with the total variation penalty, and adopted in the simulation study B-splines with 25 knots. Therefore, following Bondell et al. (2010), a sample of $n = 100$ observations is drawn from a heteroscedastic error model $y_i = f(x_i) + g(x_i)\epsilon_i$, with x_i sampled from the $U(0, 1)$ distribution and ϵ_i sampled from the $N(0, 1)$ distribution, and the following choices of mean and covariance functions:

Design 1. $f(x) = 0.5 + 2x + \sin(2\pi x - 0.5)$, $g(x) = 1$;

Design 2. $f(x) = 3x$, $g(x) = 0.5 + 2x + \sin(2\pi x - 0.5)$;

To compare the methods, 200 data sets were simulated and empirical root mean integrated squared error, $\text{RMISE} = \sqrt{1/n \sum_{i=1}^n \{Q(\tau|x_i) - \widehat{Q}(\tau|x_i)\}^2}$, and 95% (frequentist) coverage probabilities were computed for quantile levels $\tau = 0.5, 0.7, 0.9, 0.95, 0.99$. Results for Designs 1 and 2 are presented in Tables 1 and 2, respectively. Note that results for NCQR quantile estimates at $\tau = 0.5, 0.7, 0.9$ are borrowed from Bondell et al. (2010), and coverages were not reported.

Design 1 presents a simple scenario in which the variance function is constant, so quantile curves are simply parallel. From Table 1, PQPS performs similarly to NCQR in terms of RMISE, both considerably outperforming the other methods. Although coverage probabilities are not reported in Bondell et al. (2010) for NCQR, as shown in Rodrigues et al. (2016), for linear regression this estimate has coverages well below nominal level for quantiles at the tails, and similar behaviour is expected here as inference is also based on asymptotic results. Coverage probabilities for frequentist methods COBs and GCQR are also unsatisfactory for the same reason. QRJ presents nice coverage probabilities, although this current implementation evidently overfits the data, as shown in Figure 1, which illustrates estimated quantile curves for one sample from Designs 1 and 2. We

Table 1: RMISE ($\times 100$) and 95% coverage probabilities for Design 1

	0.5	0.7	0.9	0.95	0.99
<i>RMISE</i>					
PQPS	24.5	24.9	32.4	37.2	46.6
COBs	26.9	29.0	41.0	53.3	93.3
GCQR	28.6	29.7	36.2	42.5	62.1
QRJ	36.9	37.2	39.0	40.2	47.7
NCQR	25.7	25.9	31.8	-	-
<i>Coverage</i>					
PQPS	0.95	0.95	0.95	0.95	0.95
COBs	0.77	0.76	0.58	0.31	0.00
GCQR	0.95	0.95	0.92	0.82	0.49
QRJ	0.94	0.95	0.96	0.97	0.97
NCQR	-	-	-	-	-

Table 2: RMISE ($\times 100$) and 95% coverage probabilities for Design 2

	0.5	0.7	0.9	0.95	0.99
<i>RMISE</i>					
PQPS	18.5	23.0	41.6	51.4	69.3
COBs	26.7	35.9	58.2	76.2	140.4
GCQR	41.6	45.9	57.0	67.0	105.1
QRJ	55.9	64.5	89.5	105.2	146.3
NCQR	26.4	32.2	48.5	-	-
<i>Coverage</i>					
PQPS	0.97	0.97	0.94	0.92	0.90
COBs	0.85	0.77	0.62	0.42	0.00
GCQR	0.96	0.95	0.87	0.77	0.49
QRJ	0.91	0.91	0.87	0.85	0.86
NCQR	-	-	-	-	-

note that QRJ was not developed specifically for nonparametric regression, and although we tried different hyperparameters choices, no significant changes in the final fits were observed. Therefore, QRJ results throughout are preliminary and should be interpreted accordingly.

On the other hand, Design 2 brings an elaborate variance function and very distinct

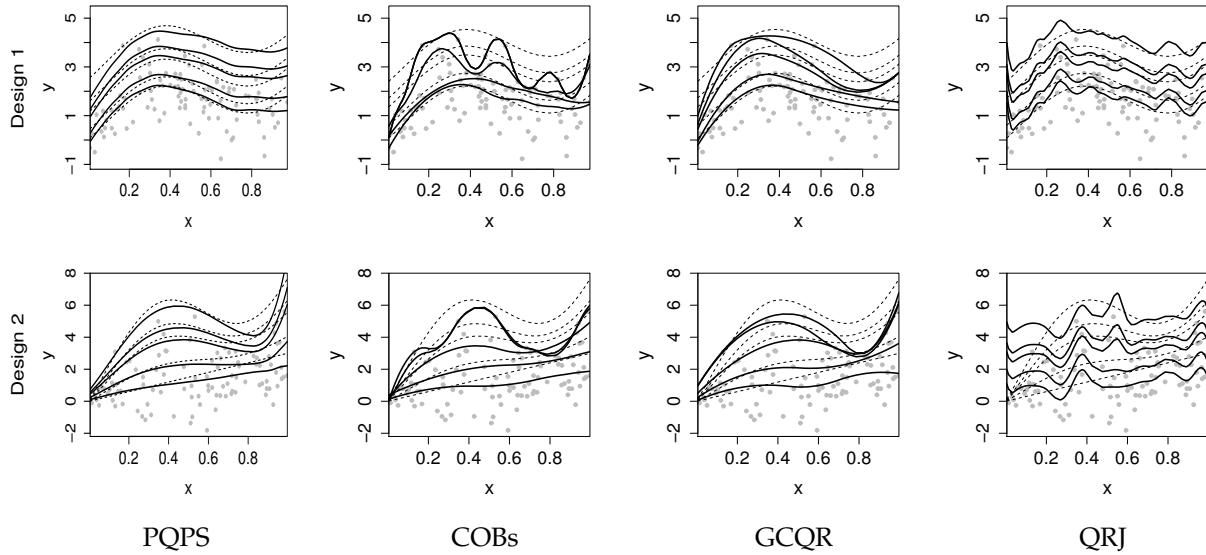


Figure 1: Estimated quantile curves at $\tau = 0.5, 0.7, 0.9, 0.95, 0.99$ for one sample from Design 1 (first row) and Design 2 (second row). Dashed lines are true quantile functions, and solid lines are quantile estimates from pyramid quantile penalised spline (PQPS), constrained B-splines (COBs), growth chart regression quantiles (GCQR) and joint estimation of linear quantile planes (QRJ).

quantile curves for each τ (see Figure 1). For this scenario, Table 2 shows that PQPS has considerably smaller RMISE than all other methods across all quantile levels, which demonstrates the flexibility of the proposed approach to fit complex quantile functions. In addition, PQPS coverage probabilities are also better than its competitors, being closer to the 95% nominal level.

For both simulation designs, Figure 1 shows severe crossings for individual quantile fitting curves from COBs, furthermore its quantile curves are clearly dissociated from one another as no borrowing information is considered. For GCQR, although quantile curves do not cross, curves are also unrelated. Indeed, when quantiles are fitted separately (or merely considering monotonicity constraints), one is discarding valuable information, which is particularly troublesome when interest also lies at the tails of the distribution, where data is already scarce. From Figure 1, we also note that the shrinkage priors used in QRJ for variable selection were incapable of discarding irrelevant covariates, so over-

fitting occurs.

Simulation Designs 3 and 4 are adapted from Smith and Kohn (1996). Here we consider a sample of $n = 100$ observations coming from

Design 3. $y = \phi(x, 0.15, 0.1^2)/4 + \phi(x, 0.6, 0.2^2)/4 + \epsilon;$

Design 4. $y = \phi(x, 0.15, 0.05^2)/4 + \phi(x, 0.6, 0.2^2)/4 + \epsilon;$

where $\phi(x, \mu, \sigma^2)$ denotes the value at x of the Normal density $\mathcal{N}(\mu, \sigma^2)$, x is an observation of $X \sim U(0, 1)$ and errors are heteroscedastic $\epsilon \sim N(0, (0.1 + x/10 + x^2/10)^2)$. While Design 3 showcases a slow varying quantile function, Design 4 presents quantile curves with degree of smoothness changing abruptly with x . This feature can easily be incorporated into our modelling framework by specifying a fat tailed distribution for the random effects parameters \mathbf{u} (Equation 10b), which are responsible for controlling the smoothness of the fit at different x . Thus, for Design 4, we assume $\mathbf{u} \sim \text{Cauchy}(\mathbf{0}, \sigma_u^2 \mathbf{I})$. One sample from each design is illustrated in Figure 2, as well as the quantile fittings from PQPS, COBs, GCQR and QRJ, all using B-splines with 20 internal knots.

From Design 4 in Figure 2, we observe that COBs quantile estimates are oversmoothed for $x < 0.4$ and undersmoothed for $x > 0.4$, as curve smoothness is assumed fixed, and an overall average smoothness is naturally not suitable here. In addition, quantile curves are dissociated from each other for COBs and GCQR, which clearly jeopardises the estimation of extreme quantiles. Notably, PQPS again exhibits the best model fit among the different methods. RMISE and 95% coverage probabilities, based on 200 simulated datasets, are presented in Tables 3 and 4.

From Tables 3 and 4, we conclude that PQPS has significantly lower RMISE for both designs and all quantile levels. COBs errors are very high for Design 4, when compared to the other methods, due to the rigid smoothness assumption. In addition, for both simulation designs, COBs coverages probabilities are well below nominal level for all quantiles. A drastic decrease is also observed for GCQR coverage probabilities at the

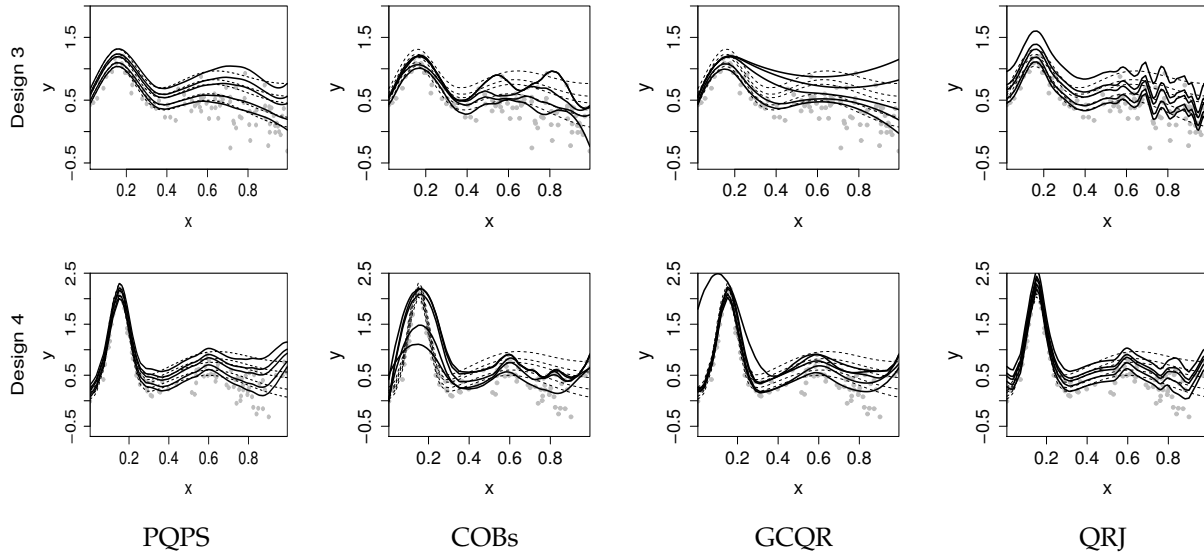


Figure 2: Estimated quantile curves at $\tau = 0.5, 0.7, 0.9, 0.95, 0.99$ for one sample from Design 3 (first row) and Design 4 (second row). Dashed lines are true quantile functions, and solid lines are quantile estimates from pyramid quantile penalised spline (PQPS), constrained B-splines (COBs), growth chart regression quantiles (GCQR) and joint estimation of linear quantile planes (QRJ).

tails. PQPS coverage is slightly under 95% for Design 4, but results are still better than the other approaches.

Table 3: RMISE ($\times 100$) and 95% coverage probabilities for Design 3

	0.5	0.7	0.9	0.95	0.99
<i>RMISE</i>					
PQPS	5.2	5.6	7.3	8.4	10.4
COBs	7.2	7.8	9.6	11.4	18.6
GCQR	6.6	7.0	9.0	10.9	18.0
QRJ	8.7	9.1	10.8	12.0	16.3
<i>Coverage</i>					
PQPS	0.97	0.96	0.96	0.96	0.96
COBs	0.55	0.53	0.46	0.24	0.00
GCQR	0.95	0.93	0.89	0.79	0.60
QRJ	0.94	0.93	0.91	0.90	0.88

In conclusion, pyramid quantile penalised spline provides a robust quantile estimate, with significantly smaller errors than all investigated methods, and also better coverages

Table 4: RMISE ($\times 100$) and 95% coverage probabilities for Design 4

	0.5	0.7	0.9	0.95	0.99
<i>RMISE</i>					
PQPS	8.1	8.4	9.9	10.9	12.9
COBs	28.2	28.0	37.0	40.3	43.4
GCQR	8.1	8.4	10.8	14.8	52.0
QRJ	8.9	9.4	11.3	12.6	16.7
<i>Coverage</i>					
PQPS	0.88	0.88	0.89	0.90	0.91
COBs	0.48	0.46	0.32	0.24	0.00
GCQR	0.97	0.96	0.88	0.81	0.55
QRJ	0.93	0.92	0.90	0.89	0.88

and model fit. In particular, the method does not drastically deteriorate in the tails. This appears to be a characteristic of the proposed procedure which adopts simultaneous fit, not only considering the noncrossing constraint.

6 Real examples

6.1 Motorcycle data set

Here we analyse the prominent motorcycle dataset (Silverman 1985). The dataset is obtained from an experiment on the efficacy of crash helmets, and contains 133 observations of head acceleration (in g) as a function of time since impact (in milliseconds). As interest lies in describing the acceleration curve, and particularly the behaviour at the tails of the distribution, quantile regression modelling is an appealing technique which has been repeatedly considered here (see Koenker 2005, Chen and Yu 2009, Pratesi et al. 2009 and Dortet-Bernadet and Fan 2012). However, all aforementioned works estimate each quantile level individually, and although quantile ordering could be imposed in a post-processing step to correct the crossing, the separate fits lose borrowing information among the quantile levels and the curves are overall dissociated from one another, as

discussed on the previous section.

We consider here the simultaneous estimation of quantile curves using smoothing B-splines with 20 internal knots. Similarly, we use an adaptive MCMC, where the covariance structure among the parameters is learnt in a first stage using 60.000 MCMC draws and burn-in of 10.000. Model parameters are estimated afterwards based on 200.000 MCMC draws, thinning every 20 samples, and 10.000 burn-in. Considering that the acceleration data presents remarkably distinct patterns of variation throughout time, with a sudden change between 10ms and 30ms lying in between very smooth trajectories (see Figure 3), we again assume a Cauchy distribution for the random effects parameters, $\mathbf{u} \sim \text{Cauchy}(\mathbf{0}, \sigma_u^2 \mathbf{I})$ (Equation 10b), in order to allow this broader range of smoothness.

Figure 3(a) shows the estimated quantile curves for PQPS at quantile levels $\tau = 0.05, 0.10, 0.25, 0.5, 0.75, 0.90, 0.95$. Estimated fits from alternative methods are also presented. Constrained B-splines (COBs) estimates quadratic splines (with L_∞ penalty) individually for each quantile level, whereas growth chart regression quantiles (GCQR) and joint quantile regression planes (QRJ) fits jointly cubic splines, with an L_2 penalty and shrinkage priors, respectively.

The proposed model for quantile regression provides a good fit to the acceleration quantile curves from the motorcycle dataset (Figure 3). PQPS quantile curves estimates are noncrossing, coherent to each other (due to the borrowing information granted by the simultaneous fit) and they nicely adapt for changes in the curve degree of smoothness. On the contrary, COBs estimates are crossing and unable to capture this varying smoothness due to the use of a global smoothness parameter, as depicted in simulation Design 4. GCRQ overall provides a reasonable fit, however there is little borrowing information among the quantile levels, so the fitted curves are dissociated from one another. As shown in the simulation studies, this is an issue for tail quantile estimation, which presents lower accuracy and coverage. The simultaneous fit provided by QRJ is noncrossing and congruent among the quantile levels, however the fit is clearly poor.

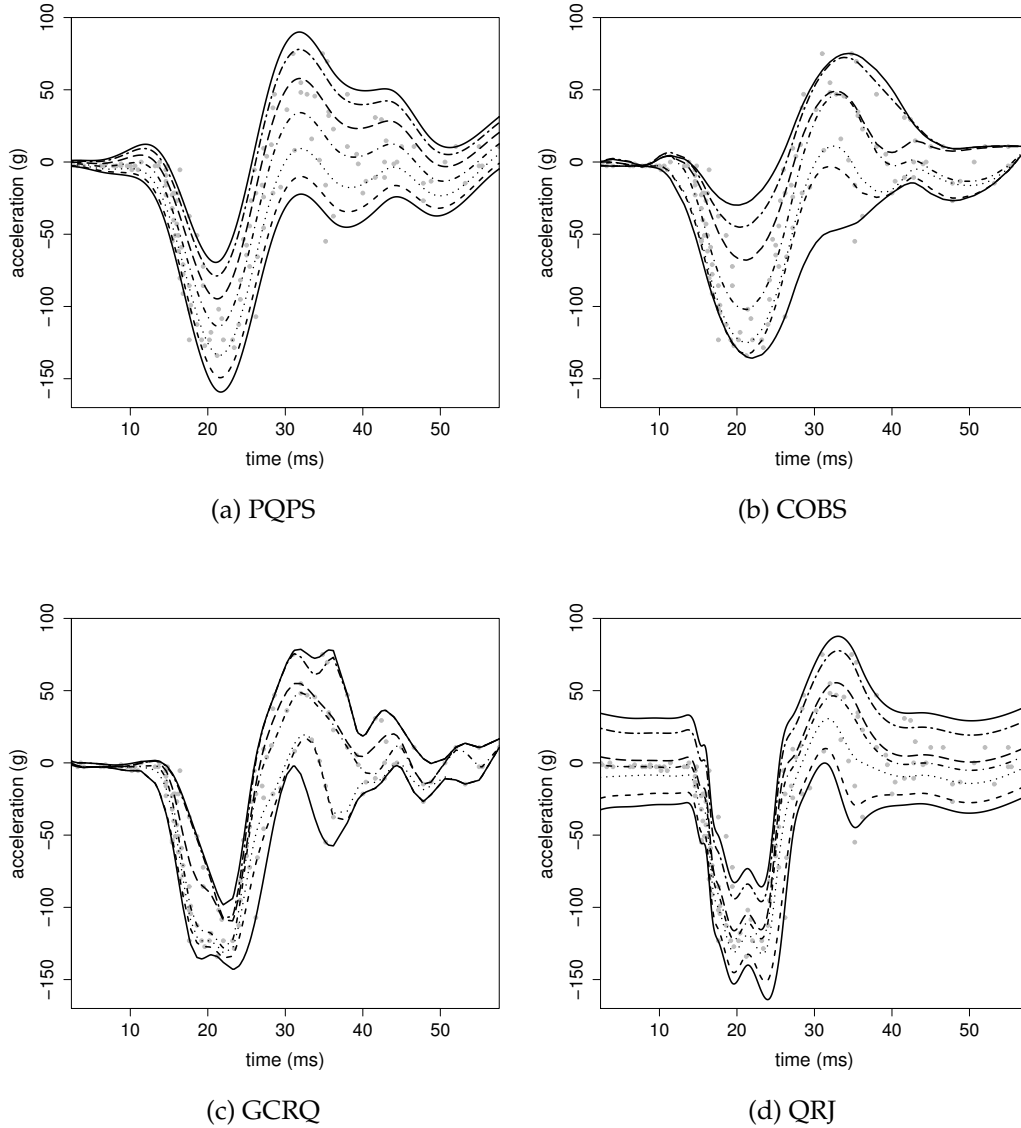


Figure 3: Estimated quantile curves for the motorcycle dataset at $\tau = 0.05, 0.10, 0.25, 0.5, 0.75, 0.90, 0.95$ from (a) PQPS: Pyramid quantile penalised spline (b) COBS: Constrained B-splines (c) GCRQ: Growth chart regression quantiles (d) QRJ: Joint estimation of linear quantile planes.

6.2 Immunoglobulin-G data set

We consider the well known dataset for analysing immunodeficiency in infants. In the search for reference ranges to help diagnose infant immunodeficiency, Isaacs et al. (1983) measured the serum concentration of immunoglobulin-G (IgG) in 298 preschool children.

As interest lies in estimating many quantiles of the response distribution, the estimates often cross. A quadratic model in age has been used previously to fit the data due to the expected smooth change of IgG with age. See Rodrigues and Fan (2017), Isaacs et al. (1983), Yu and Moyeed (2001b) and Kottas and Krnjajic (2009). For more flexibility, we consider fitting the nonparametric spline model to this dataset.

We run our proposed pyramid quantile penalised splines under similar conditions as in Section 6.1, using adaptive MCMC in a two stage procedure. The only difference is that here we used the Normal distribution for the random effects as in Equation (10b), since the smoothness here does not vary dramatically across the covariate. Figure 4 shows the fitted quantile curves at $\tau = 0.05, 0.10, 0.25, 0.5, 0.75, 0.90, 0.95$ from PQPS, COBs, GCRQ and QRJ. It is evident here that QRJ does not produce enough smoothness and provides nearly parallel curves. Both COBs and GCRQ produced similar curves to PQPS for all but the more extreme quantiles. However COBs shows wild behaviour in the two most extreme quantiles, producing crossing curves. This behaviour is also observed in earlier simulation studies for COBs. The main difference between the estimates given by GCRQ appears to be at the rightmost covariate range. Here, particularly at the higher quantile levels, GCRQ estimates suggests an increase in the IgG measurements as age increases, while both PQPS and QRJ suggest a flattening off or a small decrease. In previous simulation studies we have seen that QCRQ can perform poorly in the tails, due to the scarcity of data and not enough sharing of information across the quantiles. In this example it has lead to a rather different estimate in the higher ranges of the quantile curves.

6.3 Lidar data set

In this final example, we consider the famous heteroscedastic dataset of light detection and ranging (lidar) described in Holst et al. (1996). The dataset contains measurements of the concentration of mercury in the atmosphere, with $N = 221$ observations. As concentration depends on altitude we use the distance range, *i.e.* the distance travelled before a

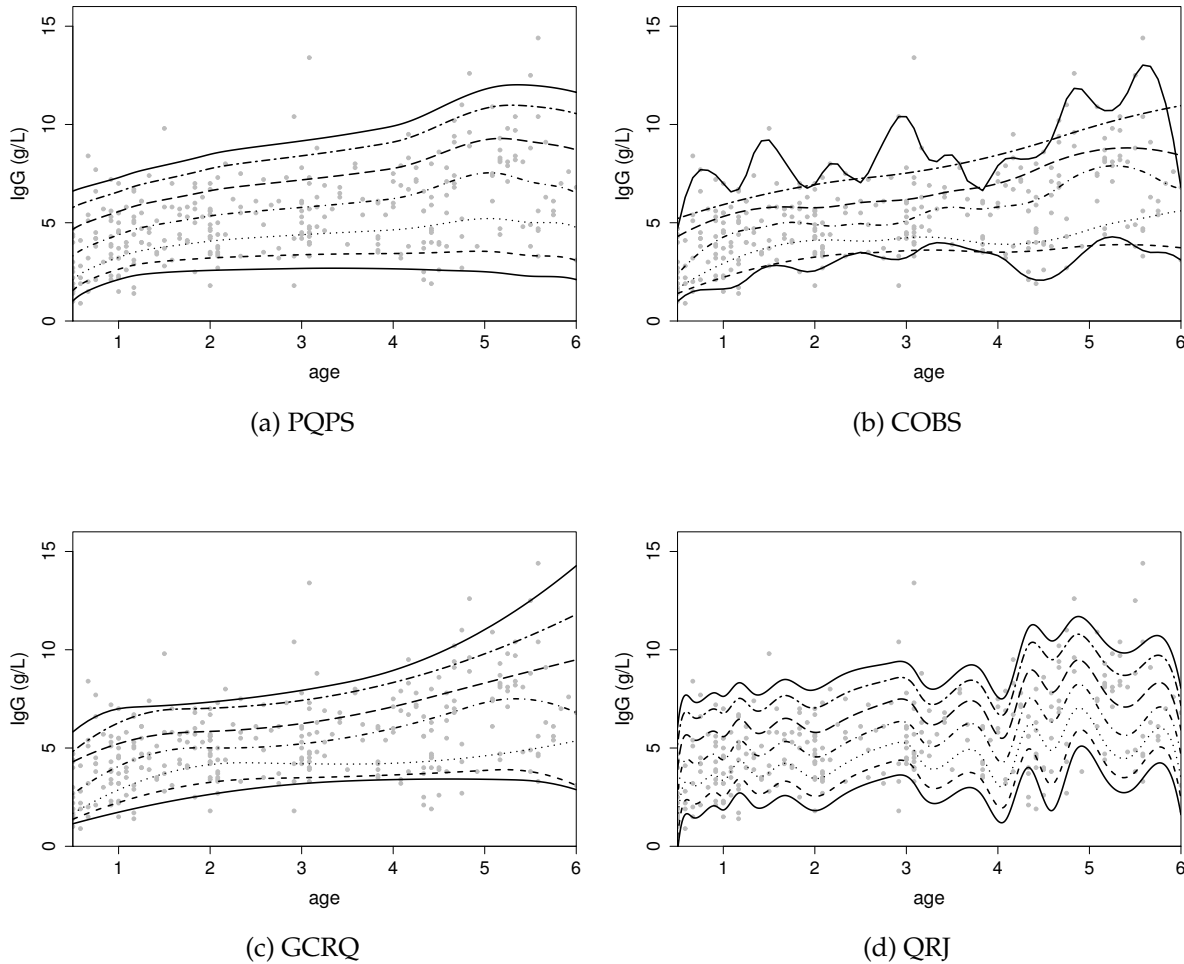


Figure 4: Estimated quantile curves for the IgG dataset at $\tau = 0.05, 0.10, 0.25, 0.5, 0.75, 0.90, 0.95$ from (a) PQPS: Pyramid quantile penalised spline (b) COBS: Constrained B-splines (c) GCRQ: Growth chart regression quantiles (d) QRJ: Joint estimation of linear quantile planes.

laser light is reflected back to its source, as covariate. The dependent variable logratio (the logarithm of the ratio of received light from two laser sources, see Ruppert et al. (1997) for more details) reflects the concentration of mercury, as they are an exact function of each other. This dataset has been frequently used to demonstrate smoothing for the mean regression curve.

We again run MCMC under the same condition as in Section 6.1, using the Cauchy distribution for the random effects parameters. Figure 5 shows the fitted quantile curves

for $\tau = 0.05, 0.10, 0.25, 0.5, 0.75, 0.90, 0.95$ using PQPS, COBS, GCRQ and QRJ. All the methods here produced visually similar results, with QRJ again not penalising enough for smoothness of the curve. While crossing does occur for this example, it is not very severe, leading to similar estimates between COBS and GCRQ. Most of the differences between the four methods of estimation appear at the leftmost of the covariate range, the COBs estimate here almost collapse to a single point, while GCRQ avoids this problem by enforcing the non-crossing constraint. Both PQPS and GCRQ perform adequately in this example, with GCRQ producing slightly more smooth estimate than PQPS.

7 Discussion

In this article, we introduced a fully nonparametric quantile regression model using the quantile pyramids. Our method uses $K + 4$ quantile pyramids to model a cubic regression spline with K knots, and places these pyramids on the vertices of an optimal convex set enclosing the predictor cloud to ensure that the fitted curves will not cross. The main features of this prior are flexibility and interpretability, as it avoids strong parametric assumptions about the data, and yet provides a straightforward construction for incorporating prior information. For instance, here we considered centring the prior on the Normal distribution, nevertheless one can easily centre it in any distribution according to prior knowledge available, or incorporate different hyperparameter modelling strategies.

The nonparametric curves were modelled using cubic B-splines with a large number of knots. Smoothing was then achieved by fitting the centring mean with O’Sullivan penalised splines. More flexibility in penalisation across quantile levels can be obtained via penalties on the scaling parameter of the centring distribution, but this was found not to be necessary in our examples. We also demonstrated with simulations and real examples that local smoothness can be easily handled by assuming a heavy tailed distribution for the random effects parameters of the mixed model formulation (Section 4.2).

A feature of our modelling approach is the simultaneous estimation of quantiles, this

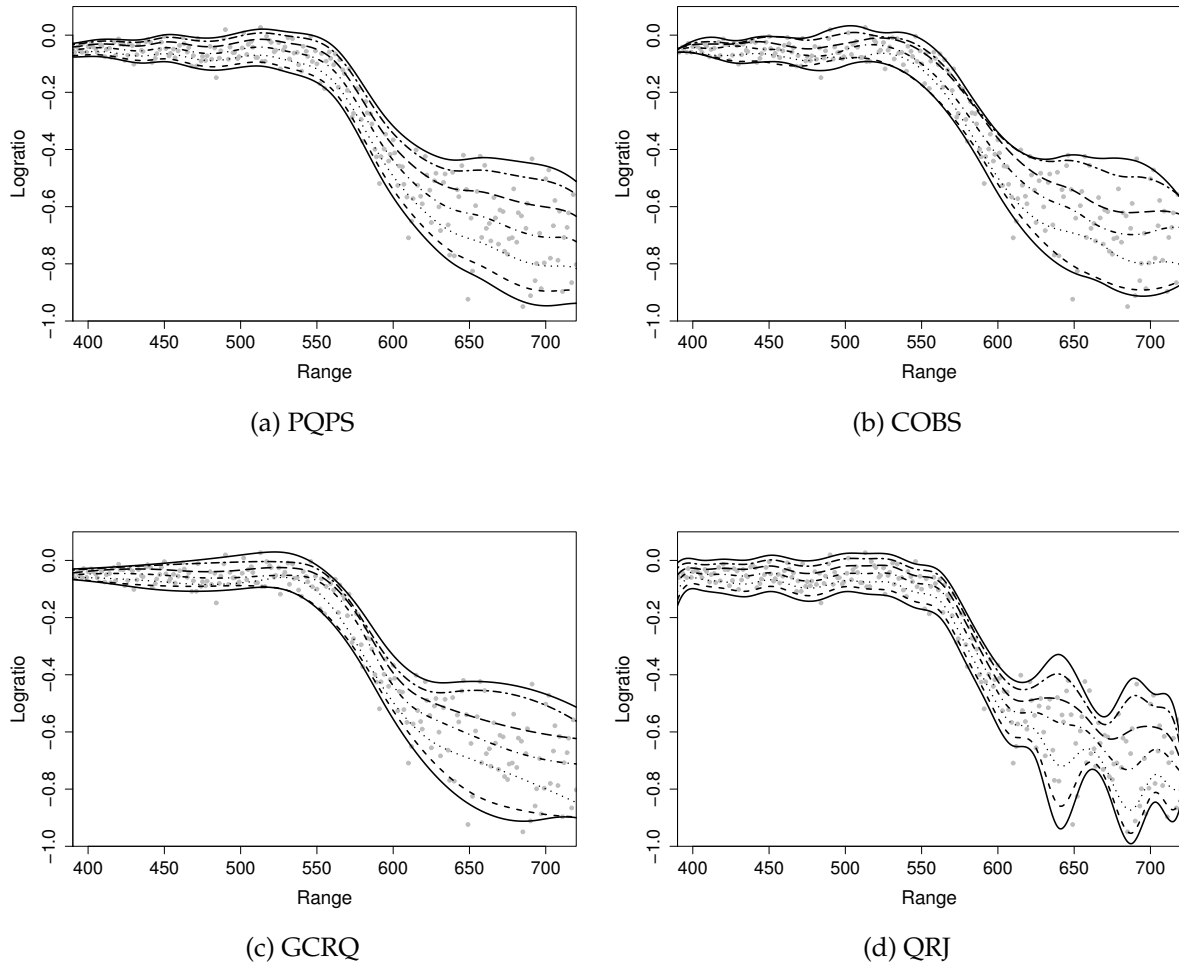


Figure 5: Estimated quantile curves for the LIDAR dataset at $\tau = 0.05, 0.10, 0.25, 0.5, 0.75, 0.90, 0.95$ from (a) PQPS: Pyramid quantile penalised spline (b) COBS: Constrained B-splines (c) GCRQ: Growth chart regression quantiles (d) QRJ: Joint estimation of linear quantile planes.

allows the sharing of information with each other. The advantage can be empirically observed, particularly in the tails of the distribution, where methods which employ simultaneous fitting hold up well into the high quantiles. Our procedure to find pyramid locations in high dimensions avoids the need to check for noncrossing constraints, allowing us to construct an effective adaptive MCMC sampling algorithm which can provide robust parameter estimates. Through simulation studies, and the analyse of real datasets, we showed that PQPS estimates have significantly smaller errors than the best available

approaches across all quantile levels, and they also provide better coverages and model fit. Extending the current framework to handle additive modelling is trivial, although the computational burden would be heavy. Computational efficiency remain an issue with the pyramid quantile approach in general, recent developments in high performance software such as RStan (RStan (2017)) and variational Bayes approaches (Han et al. (2016)), offers some encouraging future directions for improvements.

Acknowledgements

TR is funded by CAPES Foundation via the Science Without Borders (BEX 0979/13-9). TR and YF are grateful for the support of ARC ACEMS.

8 Appendix

Proof of Proposition 1. Without loss of generality, suppose that $x \in (0, 1)$. Consider the cubic splines truncated power basis

$$1, x, x^2, x^3, (x - \gamma_1)_+^3, (x - \gamma_2)_+^3, \dots, (x - \gamma_K)_+^3$$

with K knots $0 < \gamma_1 < \gamma_2 < \dots < \gamma_K < 1$. Also, let

$$\mathcal{X} = \{(x, x^2, x^3, (x - \gamma_1)_+^3, \dots, (x - \gamma_K)_+^3), x \in (0, 1)\}$$

be the corresponding one-dimensional curve in \mathbb{R}^{K+3} . We consider finding $K+4$ locations in \mathbb{R}^{K+3} whose convex hull encloses, as narrowly as possible, this curve \mathcal{X} . The following steps describe the selection of the tightest region using tangent planes.

First, we consider the first three elements of the basis, $1, x$ and x^2 , with corresponding curve $\mathcal{X}_1 = \{(x, x^2), x \in (0, 1)\}$ in \mathbb{R}^2 . To enclose this curve we set some pyramid locations at its two extremities, say $x_1^1 = (0, 0)$ and $x_1^3 = (1, 1)$. For the remaining location, we note

that the smallest triangle enclosing \mathcal{X}_1 is obtained when its sides are tangent to \mathcal{X}_1 at x_1^1 and x_1^3 . Calculating the intersection of the two tangent lines to the curve at x_1^1 and x_1^3 and we get $x_1^2 = (\frac{1}{2}, 0)$. See Figure 6a.

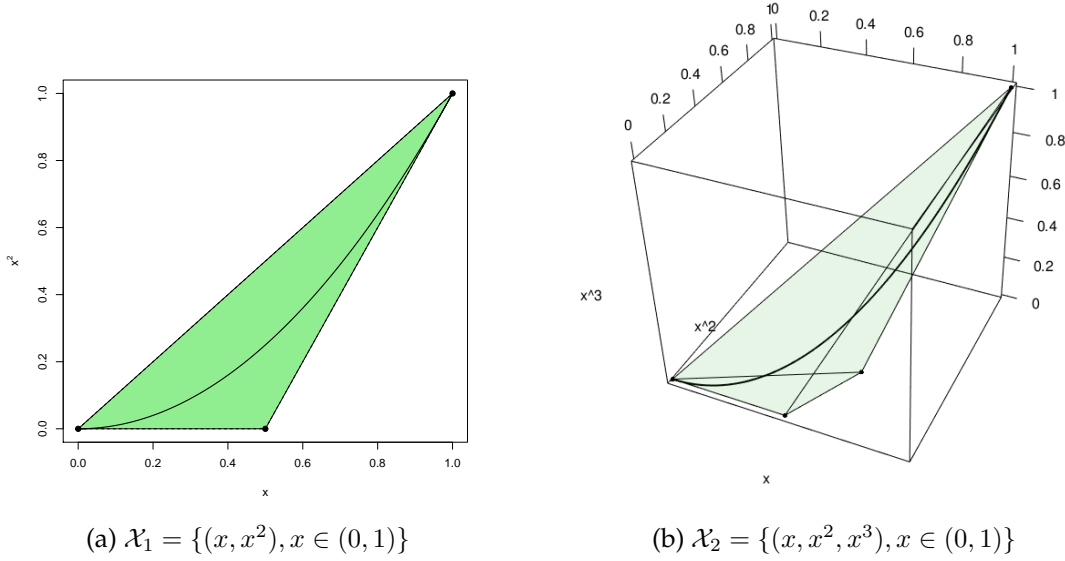


Figure 6: Pyramid locations for the basis $\{1, x, x^2\}$ (a) and $\{1, x, x^2, x^3\}$ (b). The pyramid locations are given by the dots, the corresponding convex hull are the shaded regions enclosing the curves $\mathcal{X}_1 = \{(x, x^2), x \in (0, 1)\}$ and $\mathcal{X}_2 = \{(x, x^2, x^3), x \in (0, 1)\}$.

At the second step, we consider the first four elements of the basis and the corresponding curve in \mathbb{R}^3 , $\mathcal{X}_2 = \{(x, x^2, x^3), x \in (0, 1)\}$. To enclose this curve, again, we set two pyramid locations at its extremities, $x_2^1 = (0, 0, 0)$ and $x_2^4 = (1, 1, 1)$. Let (x, y, z) be the Cartesian coordinates in \mathbb{R}^3 . Since the derivative of the curve at x_2^1 is $(1, 0, 0)'$ we know that the two remaining pyramid locations are on the plane $\{z = 0\}$. Since the mapping of \mathcal{X}_2 onto this plane is \mathcal{X}_1 , we re-use the pyramid location defined at first step, $x_2^2 = (\frac{1}{2}, 0, 0)$. For the last pyramid location, we calculate the intersection of the line given by the derivative of the curve at x_2^4 with the plane $\{z = 0\}$. The line has equation $\{(x, y, z)' = (1, 1, 1)' + t(1, 2, 3)', t \in \mathbb{R}\}$, thus we get $x_2^3 = (\frac{2}{3}, \frac{1}{3}, 0)$. See Figure 6b.

For the next step, we introduce in the basis the truncated cubic function $(x - \gamma_1)_+^3$ for a knot $0 < \gamma_1 < 1$. To enclose the corresponding curve $\mathcal{X}_3 = \{(x, x^2, x^3, (x - \gamma_1)_+^3), x \in (0, 1)\}$, we proceed as before: two pyramid locations are set at the extremities of the curve, $x_3^1 =$

$(0, 0, 0, 0)$ and $x_3^5 = (1, 1, 1, (1 - \gamma_1)^3)$, and we re-use the pyramid locations previously defined, now $x_3^2 = (\frac{1}{2}, 0, 0, 0)$ and $x_3^3 = (\frac{2}{3}, \frac{1}{3}, 0, 0)$. The only new pyramid location to calculate lies at the intersection of the line given by the derivative of the curve at x_3^5 with the hyperplane $\{(x, y, z, 0), (x, y, z) \in \mathbb{R}^3\}$ of \mathbb{R}^4 . The line has equation $\{(x, y, z, w)' = (1, 1, 1, (1 - \gamma_1)^3)' + t(1, 2, 3, 3(1 - \gamma_1)^2)', t \in \mathbb{R}\}$, and setting the last coordinate to 0 we get $x_3^4 = (\frac{2+\gamma_1}{3}, \frac{1+2\gamma_1}{3}, \gamma_1, 0)$.

New truncated cubic functions can be added to the basis by induction. Suppose we want to add to the basis $1, x, x^2, (x - \gamma_1)_+^3, \dots, (x - \gamma_{K-1})_+^3$ the function $(x - \gamma_K)_+^3$, we then re-use the pyramid locations previously defined, and calculate the only new pyramid location. For that, we first determine the line given by the derivative of \mathcal{X} at $x^{K+4} = (1, 1, 1, (1 - \gamma_1)^3, \dots, (1 - \gamma_K)^3)$,

$$\{(1 + t, 1 + 2t, 1 + 3t, (1 - \gamma_1)^3 + 3t(1 - \gamma_1)^2, \dots, (1 - \gamma_K)^3 + 3t(1 - \gamma_K)^2), t \in \mathbb{R}\},$$

then setting its last coordinate to 0, we get

$$x^{K+3} = \left(\frac{2+\gamma_K}{3}, \frac{1+2\gamma_K}{3}, \gamma_K, (\gamma_K - \gamma_1)(1 - \gamma_1)^2, (\gamma_K - \gamma_2)(1 - \gamma_2)^2, \dots, (\gamma_K - \gamma_{K-1})(1 - \gamma_{K-1})^2, 0 \right).$$

□

References

- Bondell, H. D., B. J. Reich, and H. Wang (2010). Noncrossing quantile regression curve estimation. *Biometrika* 97(4), 825–838.
- Bosch, R. J., Y. Ye, and G. G. Woodworth (1995). A convergent algorithm for quantile regression with smoothing splines. *Computational Statistics & Data Analysis* 19(6), 613 – 630.

- Cade, B. S., J. W. Terrell, and R. L. Schroeder (1999). Estimating effects of limiting factors with regression quantiles. *Ecology* 80(1), 311–323.
- Chen, C. and K. Yu (2009). Automatic Bayesian quantile regression curve fitting. *Statistics and Computing* 19, 271–281.
- Chernozhukov, V., I. Fernandez-Val, and A. Galichon (2009). Improving point and interval estimators of monotone functions by rearrangement. *Biometrika* 96, 559–575.
- Dette, H. and S. Volgushev (2008). Non-crossing non-parametric estimates of quantile curves. *Journal of Royal Statistical Society B* 70, 609–627.
- Dortet-Bernadet, J.-L. and Y. Fan (2012). On Bayesian quantile regression curve fitting via auxiliary variables. arXiv:1202.5883v1[stat.ME].
- Fang, Y., Y. Chen, and X. He (2015). Bayesian quantile regression with approximate likelihood. *Bernoulli* 21(2), 832–580.
- Fitzenberger, B., R. Koenker, and J. A. F. Machado (2002). *Economic Applications of Quantile Regression*. Physica.
- Garthwaite, P. H., Y. Fan, and S. A. Sisson (2016). Adaptive optimal scaling of metropolis-hastings algorithms using the robbins-monro process. *Communications in Statistics - Theory and Methods* 45, 5098–5111.
- Han, S., X. Liao, D. B. Dunson, and L. Carin (2016). Variational gaussian copula inference. In *19th International Conference on Artificial Intelligence and Statistics*, Volume 51, pp. 829 – 838.
- Hastie, T. J. and R. J. Tibshirani (1990). *Generalised additive models*. Chapman and Hall, London.
- He, X. (1997). Quantile curves without crossing. *American Statistician* 51, 186–192.
- He, X. and P. Ng (1999). Cobs: Qualitatively constrained smoothing via linear programming. *Computational Statistics* 14(3), 315–337.

- Hjort, N. L. and S. G. Walker (2009). Quantile pyramids for Bayesian nonparametrics. *Annals of Statistics* 37(1), 105–131.
- Holst, U., O. Hossjer, C. Bjorklund, P. Ragnarson, and H. Edner (1996). Locally weighted least squares kernel regression and statistical evaluation of lidar measurements. *Environmetrics* 7, 401–416.
- Isaacs, D., D. G. Altman, C. E. Tidmarsh, H. B. Valman, and A. D. B. Webster (1983). Serum immunoglobulin concentration in preschool children measured by laser nephelometry: reference ranges for IgG, IgA, IgM. *Journal of Clinical Pathology* 36, 1193–1196.
- Koenker, R. (2005). *Quantile regression*, Volume 38 of *Econometric Society Monographs*. Cambridge: Cambridge University Press.
- Koenker, R. and J. Bassett, Gilbert (1978). Regression quantiles. *Econometrica* 46(1), 33–50.
- Koenker, R., P. Ng, and S. Portnoy (1994). Quantile smoothing splines. *Biometrika* 81(4), 673.
- Kottas, A. and M. Krnjajic (2009). Bayesian semiparametric modelling in quantile regression. *Scandinavian Journal of Statistics* 36, 297–319.
- Muggeo, V. M. R., M. Sciandra, A. Tomasello, and S. Calvo (2013). Estimating growth charts via nonparametric quantile regression: a practical framework with application in ecology. *Environmental and Ecological Statistics* 20(4), 519–531.
- Ng, P. and M. Maechler (2007). A fast and efficient implementation of qualitatively constrained quantile smoothing splines. *Statistical Modelling* 7(4), 315–328.
- Ng, P. T. and M. Maechler (2015). *COBS – Constrained B-splines (Sparse matrix based)*. R package version 1.3-1.
- Portnoy, S. (2003). Censored regression quantiles. *Journal of the American Statistical As-*

- sociation* 98(464), 1001–1012.
- Pratesi, M., M. G. Ranalli, and N. Salvati (2009). Nonparametric m-quantile regression using penalised splines. *Journal of Nonparametric Statistics* 21(3), 287–304.
- Reich, B. J., M. Fuentes, and D. B. Dunson (2011). Bayesian spatial quantile regression. *Journal of the American Statistical Association* 106(493), 6–20.
- Reich, B. J. and L. B. Smith (2013). Bayesian quantile regression for censored data. *Biometrics* 69, 651–660.
- Roberts, G. O., A. Gelman, and W. R. Gilks (1997, 02). Weak convergence and optimal scaling of random walk metropolis algorithms. *Ann. Appl. Probab.* 7(1), 110–120.
- Roberts, G. O. and J. S. Rosenthal (2001). Optimal scaling for various Metropolis-Hastings algorithms. *Statistical Science* 16, 351–367.
- Rodrigues, T., J.-L. Dortet-Bernadet, and Y. Fan (2016). Pyramid quantile regression. arXiv:1606.05407 [stat.ME].
- Rodrigues, T. and Y. Fan (2017). Regression adjustment for noncrossing Bayesian quantile regression. *Journal of Computational and Graphical Statistics* 26, 275–284.
- RStan (2017). Stan development team, RStan: the R interface to Stan. R package version 2.16.2.
- Ruppert, D., M. Wand, and R. Carroll (2003). *Semiparametric Regression*. Cambridge University Press.
- Ruppert, D., M. P. Wand, U. Holst, and O. Hössjer (1997). Local polynomial variance function estimation. *Technometrics* 39(3), 262–273.
- Silverman, B. W. (1985). Some aspects of the spline smoothing approach to nonparametric regression curve fitting. *Journal of the Royal Statistical Society. Series B (Methodological)* 47(1), 1–52.

- Smith, M. and R. Kohn (1996). Nonparametric regression using bayesian variable selection. *Journal of Econometrics* 75(2), 317 – 343.
- Spiriti, S., R. Eubank, P. W. Smith, and D. Young (2013). Knot selection for least-squares and penalized splines. *Journal of Statistical Computation and Simulation* 83(6), 1020–1036.
- Statisticat and LLC. (2016). *LaplacesDemon: Complete Environment for Bayesian Inference*. R package version 16.0.1.
- Thompson, P., Y. Cai, R. Moyeed, D. Reeve, and J. Stander (2010). Bayesian nonparametric quantile regression using splines. *Computational Statistics and Data Analysis* 54(4), 1138 – 1150.
- Tokdar, S. (2016). *qrjoint: Joint Estimation in Linear Quantile Regression*. R package version 1.0-0.
- Wand, M. P. and J. T. Ormerod (2008). On semiparametric regression with o’sullivan penalized splines. *Australian & New Zealand Journal of Statistics* 50(2), 179–198.
- Yang, Y. and S. Tokdar (2017). Joint estimation of quantile planes over arbitrary predictor spaces. *Journal of the American Statistical Association* 112(1107-1120).
- Yu, K. and R. A. Moyeed (2001a). Bayesian quantile regression. *Statist. Probab. Lett.* 54(4), 437–447.
- Yu, K. and R. A. Moyeed (2001b). Bayesian quantiles regression. *Statistics and Probability Letters* 54, 437–447.